 doi:10.20944/preprints202107.0142.v1

*Article*

# Jasmonic acid-dependent MYC transcription factors bind to a tandem G-box motif in the *YUCCA8* and *YUCCA9* promoters to regulate biotic stress responses

**Marta-Marina Pérez-Alonso[1,2]*, Beatriz Sánchez-Parra[1,3], Paloma Ortíz-García[1], M. Estrella Santamaria[1,4], Isabel Diaz[1,4], Stephan Pollmann[1,4]***

[1] Centro de Biotecnología y Genómica de Plantas, Universidad Politécnica de Madrid (UPM)-Instituto nacional de Investigación y Tecnología Agraria y Alimentación (INIA), Pozuelo de Alarcón, 28223, Spain.
[2] Department of Forest Genetics and Plant Physiology, Umeå Plant Sciences Centre (UPSC), Swedish University of Agricultural Science, 90183, Umeå, Sweden.
[3] Institut für Biologie, Bereich Pflanzenwissenschaften, Karl-Franzens Universität Graz, 8010, Graz, Austria.
[4] Departamento de Biotecnología-Biología Vegetal, Escuela Técnica Superior de Ingeniería Agronómica, Alimentaria y de Biosistemas, Universidad Politécnica de Madrid (UPM), 28040, Madrid, Spain.

* Correspondence: Stephan Pollmann (S.P.), stephan.pollmann@upm.es, Tel.: +34-910679183; Marta-Marina Pérez Alonso (MM.PA.), marta.perez.alonso@slu.se

**Abstract:** The indole-3-pyruvic acid pathway is the major route for auxin biosynthesis in higher plants. Tryptophan aminotransferases (TAA1/TAR) and members of the YUCCA family of flavin-containing monooxygenases catalyze the conversion of L-tryptophan via indole-3-pyruvic acid into indole-3-acetic acid (IAA). It has been described that locally produced jasmonic acid (JA) in response to mechanical wounding, triggers *de novo*-formation of IAA through the induction of two *YUCCA* genes, *YUC8* and *YUC9*. Here, we report the direct involvement of a small number of basic helix-loop-helix transcription factors of the MYC family in this process. We show that the JA-mediated regulation of *YUC8* and *YUC9* gene expression depends on the abundance of MYC2, MYC3, and MYC4. In support of this observation, seedlings of *myc* knockout mutants displayed a strongly reduced response to JA-mediated IAA formation. In addition, transactivation assays provided experimental evidence for the binding of the MYC transcription factors to a particular tandem G-box motif abundant in the promoter regions of *YUC8* and *YUC9*, but not in those of the other *YUCCA* genes. Moreover, we clearly demonstrate that YUC8ox and YUC9ox overexpressing plants show less damage after spider mite infestation, thereby underlining a role of auxin in plant responses toward biotic stress cues.

**Keywords:** *Arabidopsis thaliana*, indole-3-acetic acid, jasmonic acid, plant hormone crosstalk, transcriptional regulation, wound response, biotic stress, growth-defense trade-off

## 1. Introduction

Since its discovery in the thirties of the last century [1-3], many genetic and biochemical studies clearly demonstrated that auxins govern virtually every aspect of plant life, related

Preprints (www.preprints.org) | NOT PEER-REVIEWED | Posted: 6 July 2021 doi:10.20944/preprints202107.0142.v1

with growth and development, *i.e.* cell division, cell elongation, cell differentiation, tropisms, apical dominance, emergence of new primordia, initiation of lateral and adventitious root growth, senescence, leaf abscission, and flowering [4-6]. However, despite the tremendous importance of auxins for plant development, the role of auxin in plant defense is still not fully understood. Several lines of evidence indicate that indole-3-acetic acid (IAA), the major auxin in plants, exerts a negative role in plant stress resistance, and that investing in plant growth imposes a penalty on plant defense, and *vice versa* [7-10]; a phenomenon referred to as the growth-defense trade-off [11]. In line with these affirmations, it has been described that activation of IAA mediated stem elongation in response to light, increases the susceptibility of *Arabidopsis thaliana* and *Chenopodium album* to different pathogens, such as the bacteria *Pseudomonas syringae* or the herbivore *Spodoptera exigua* [12,13]. Likewise, Mutka and co-workers (2013) showed that elevation of endogenous IAA levels in Arabidopsis decreases plant tolerance against *P. syringae*. Conversely, another series of studies suggests that auxin can positively influence plant tolerance. For example, it has been demonstrated that the auxin signaling component AUXIN RESPONSE FACTOR3 (ARF3) controls the formation of leaf trichomes, considered a direct defense mechanism against predators [15,16]. In addition, analysis carried out using the Arabidopsis auxin reporter line DR5::GUS showed that mechanical wounding stimulates IAA signaling in neighboring unwounded plants [17], which suggests an indirect defense mechanism that allows plants to get prepared for a possible imminent attack. Taking all together, we intend not only to shed light on the implication of auxin in plant biotic stress responses, but also to provide new molecular targets that mediate the trade-off between plant growth and defense.

In this context, jasmonates play a prominent role. Jasmonates are a group of lipid-derived hormones comprising jasmonic acid (JA) and several JA derivatives [18]. These molecules have an essential role in counteracting abiotic and biotic stress responses, such as pathogen and herbivore attack [19-21]. Upon stress recognition, the production of the bioactive JA, jasmonoyl-L-isoleucine (JA-Ile) is stimulated and perceived by the protein CORONATINE INSENSITIVE 1 (COI1). This enables the Skp-cullin 1-F-box (SCF) E3 ligase complex to bind and ubiquitinate specific repressor proteins called JASMONATE ZYM DOMAIN (JAZ). Degradation of JAZs by the 26S proteosome releases the MYC family of basic helix-loop-helix (bHLH) transcription factors from repression, which subsequently triggers the expression of different subsets of JA-responsive genes [11], [22,23].

Over the past few years, a wide array of links between JA and auxin signaling pathways has been reported. For instance, JA has been demonstrated to negatively affect primary root growth in *A. thaliana* through the transcriptional repression of *PLETHORA* genes expression, namely of *PLT1* and *PLT2*, which are known as essential transcription factors controlling auxin-regulated root meristem specification and maintenance [24]. A more recent work described a crosstalk model in which wound-inducible amidohydrolases contribute to the cellular regulation of JA and auxin levels to coordinate stress responses by controlling JA- and IAA-amino acid conjugate contents [16]. In contrast, a series of

Preprints (www.preprints.org) | NOT PEER-REVIEWED | Posted: 6 July 2021 doi:10.20944/preprints202107.0142.v1

publications emphasized that JA exerts a direct stimulating effect on various phases of auxin biosynthesis. Dombrecht *et al*. (2007) reported that the JA-associated transcription factor MYC2 controls the formation of auxin biosynthesis precursors as well as auxin-related defense compounds, such as indole glucosinolates. Furthermore, JA has been shown to promote auxin *de novo*-biosynthesis through the transcriptional activation of two anthranilate synthase genes, *ASA1* and *ASB1*, resulting in elevated L-tryptophan levels and, thus, increased precursor availability for auxin biosynthesis [26]. A more direct impact on auxin biosynthesis has been reported by Hentrich *et al*. (20013) . The authors provided evidence for the JA-dependent transcriptional activation of two Arabidopsis *YUCCA* genes, *YUC8* and *YUC9*. Intriguingly, YUCCA enzymes are considered key players in general IAA biosynthesis, along with tryptophan aminotransferases [28-31]. Importantly, the gene expression studies presented by Hentrich *et al.* (2013a) demonstrated that the *YUC8* and *YUC9* transcriptional response towards the treatment with different oxylipins, such methyl jasmonate (MeJA) and its precursor 12-oxo-phytodienoic acid (OPDA), is almost entirely impaired in the *coi1* mutant background. Based on this experiment, it can be speculated that the transcriptional regulation of *YUC8* and *YUC9* depends on the COI-JAZ-MYC signaling module.

In this work, we show that the Arabidopsis transcription factor MYC2, and its closest homologs MYC3 and MYC4 [32], play a direct role in the regulation of auxin biosynthesis trough the control of *YUC8* and *YUC9* gene expression. We demonstrate that different *myc* knockout mutants display a significant reduction not only in JA-mediated IAA production, but also in *YUC8* and *YUC9* transcript accumulation. Moreover, our transient transactivation analyses in *Nicotiana benthamiana* and Arabidopsis protoplasts clearly demonstrate that MYC2, MYC3 and MYC4 bind to a specific tandem G-box motif abundant in the promoter regions of *YUC8* and *YUC9*, which is not abundant in those of the other *YUCCA* genes. Finally, *YUC8* and *YUC9* mutants have been exposed to the two-spotted spider mite *Tetranychus urticae*, which provided compelling evidence that the overexpression of the two genes rendered the mutant plants more resistant toward herbivore predators. Taken together, these results provide evidence for a signal transduction mechanism that employs the COI-JAZ-MYC module to fine-tune the expression of auxin biosynthesis-related genes in response to wounding and resistance to phytophagous mites.

## 2. Results

### The jasmonate signaling components MYC2, MYC3 and MYC4 are required for auxin formation after JA treatment

Firstly, we investigated whether MYC transcription factors are directly involved in *de novo* IAA synthesis. To this end, we quantified the endogenous IAA levels in *A. thaliana* wild-type seedlings (Col-0), as well as different *myc* knockout mutants, 4 h after the treatment with 50 μM MeJA by gas chromatography-tandem mass spectrometry (GC-MS/MS) (Figure 1). Confirming previous observations [27], application of MeJA to WT seedlings

Preprints (www.preprints.org) | NOT PEER-REVIEWED | Posted: 6 July 2021 doi:10.20944/preprints202107.0142.v1

resulted in more than 5-fold enhanced IAA formation relative to mock-treated control seedlings (0.5% MeOH (v/v)). In contrast, the IAA production in response to MeJA-treatment appeared to be clearly impaired in all *myc* single mutants, as well as in the *myc2*/*myc3* and *myc2*/*myc4* double and *myc2*/*myc3*/*myc4* triple mutants. The strongest effect was visible in the triple mutant, displaying a 0.5-fold reduction of IAA levels in comparison to the respective mock-treated control. The additive effect observed in the triple mutant indicates that MYC2, MYC3 and MYC4 transcription factors collaborate in the control of JA-mediated IAA accumulation. Remarkably, although all single *myc* mutants displayed a general tendency of impaired MeJA-mediated IAA formation (no significant differences to the mock-treated controls), *myc3*/*myc4* seedlings exhibited a remaining significant increase in IAA contents in response to the MeJA application. However, with an increase of approximately 3.5-fold over the corresponding mock-treated *myc3*/*myc4* seedlings, the exhibited response was still weaker than the one detected for wild-type seedlings.

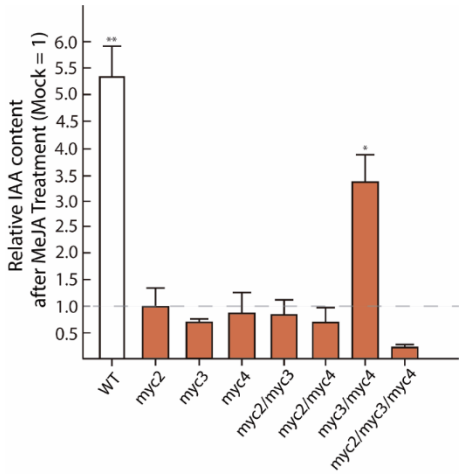


**Figure 1.** JA-mediated IAA biosynthesis is impaired in several Arabidopsis *myc* knockout mutants. IAA levels were measured by GC-MS/MS in 10 days-old seedlings treated with 50 µM MeJA or mock solution (0.5% MeOH (v/v)) for 4h. The IAA accumulation was calculated as a ratio of the endogenous IAA to the stable isotope-labelled [$^2H_2$]-MeIAA. Then, the final relative IAA content is given by the difference of auxin levels in each MeJA treated sample and the respective control and expressed as pmol IAA per gram fresh weight. The levels of samples without MeJA treatment (0.5% MeOH (v/v)) were arbitrarily set to 1. Values are mean ± SE (n = 3). Statistical analysis was performed using Student's *t*-test comparing the mock treated seedlings with the respective MeJA treated WT or *myc* loss-of-function mutant. Significant differences between means are indicated with asterisk (*P < 0.05, **P < 0.01).

In summary, the presented results support the hypothesis of an intimate crosstalk between JA signaling and IAA biosynthesis. At the same time, the obtained data suggest a leading role of MYC2 in this process.

### *YUC8* and *YUC9* expression is suppressed in *myc* loss-of-function mutants

To evaluate the role of MYC transcription factors in the transcriptional activation of *YUC8* and *YUC9*, we conducted quantitative reverse transcriptase PCR (qRT-PCR) analyses after

Preprints (www.preprints.org) | NOT PEER-REVIEWED | Posted: 6 July 2021 doi:10.20944/preprints202107.0142.v1

seedlings were treated with exogenous MeJA. In line with the results presented above, we observed that the abundance of *YUC8* and *YUC9* transcripts increased 1.3-fold and 8.7-fold in WT seedlings respectively (Figure 2). Moreover, we found that the gene expression of both *YUC* genes was unaffected by MeJA treatment in practically all single, double, and triple *myc* knockout mutants, relative to the respective mock treated seedlings. Surprisingly, in both *myc3* and *myc2myc3* the *YUC8* transcription was slightly induced after 4 h of MeJA treatment (0.67-fold induction and 1.4-fold induction, respectively) (Figure 2A). Likewise, in the *myc4* background *YUC9* expression was highly induced after 2h of MeJA application (7.8-fold induction) (Figure 2B). In summary, these data highlight that *YUC8* transcription is driven by MYC2 and MYC4. While MYC2 and MYC3 act as major regulators of *YUC9* gene expression in response to oxylipins. It is noteworthy that, when studying the *myc2myc3myc4* triple mutant, we did not observe a complete suppression of the *YUC8* and *YUC9* transcription (Figure 2A,B). This observation may be interpreted as an indication for a compensatory mechanism to attenuate the absence of JA response in plants.

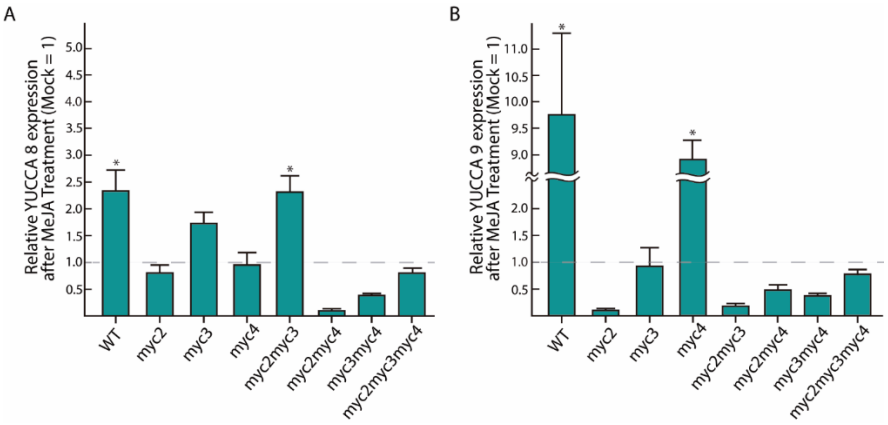


**Figure 2.** MY2, MYC3 and MYC4 control *YUC8* and *YUC9* gene expression in response to MeJA. (**A**) Quantitative RT-PCR analysis of *YUC8* after 4 h of MeJA induction treatment. (**B**) *YUC9* expression levels after 2 h of MeJA treatment. Both *YUC8* and *YUC9* transcript levels are given relative to the reference genes *APT1* and *UBI10* and normalized using the mock treated seedlings (0.5% MeOH (v/v)). Data shown are mean ± SE (n = 3). A two-fold change between the control mock treated seedlings and the respective *myc* ko mutant was considered as differentially regulated (* fold-change ≥ 2).

### *In silico* analysis of *YUCCA* promoter sequences indicates a conserved MYC2, MYC3 and MYC4 binding sites in the promoter of *YUC8* and *YUC9*

To further confirm the role of MYC2, MYC3 and MYC 4 in the transcriptional regulation of *YUC8* and *YUC9*, the 3000 bp sequence upstream of the transcription start was isolated for each *A. thaliana YUCCA* gene and used to predict MYC binding motifs, *i.e.*, G-box and sixteen described G-box variants [32] . As shown in Figure 3, we observed that the jasmonate responsive elements, G-box and G-box variants, are highly enriched in all *YUCCA* promoter sequences. However, we detected that only pYUC8 and pYUC9 contain a specific "tandem" DNA binding motif configuration. This "tandem" includes two

 doi:10.20944/preprints202107.0142.v1

canonical G-boxes (5'-CACGTG-3') and one G-box variant 9 (5'-CACGTC-3') at the nucleotide positions -535, -555 and -571 in case of pYUC8, and -1240, -1247 and -1272 in pYUC9. In addition, we found that this configuration is followed by the G-box variant 3 (5'-CATGTG -3') in positions -140 and -207 of pYUC8 and pYUC9, respectively. Remarkably, the G-box variant 3 was relatively close to a 5'-TATAAA-3' sequence, in positions -153 (pYUC8) and -267 (pYUC9). This sequence was identified as the consensus TATA-box, which is commonly recognized as a transcription enhancer [33]. In conclusion, the prediction of putative *cis*-elements prompted us to hypothesize that this G-box configuration may be crucial for the transcriptional regulation of both *YUC8* and *YUC9*.

Preprints (www.preprints.org) | NOT PEER-REVIEWED | Posted: 6 July 2021 doi:10.20944/preprints202107.0142.v1

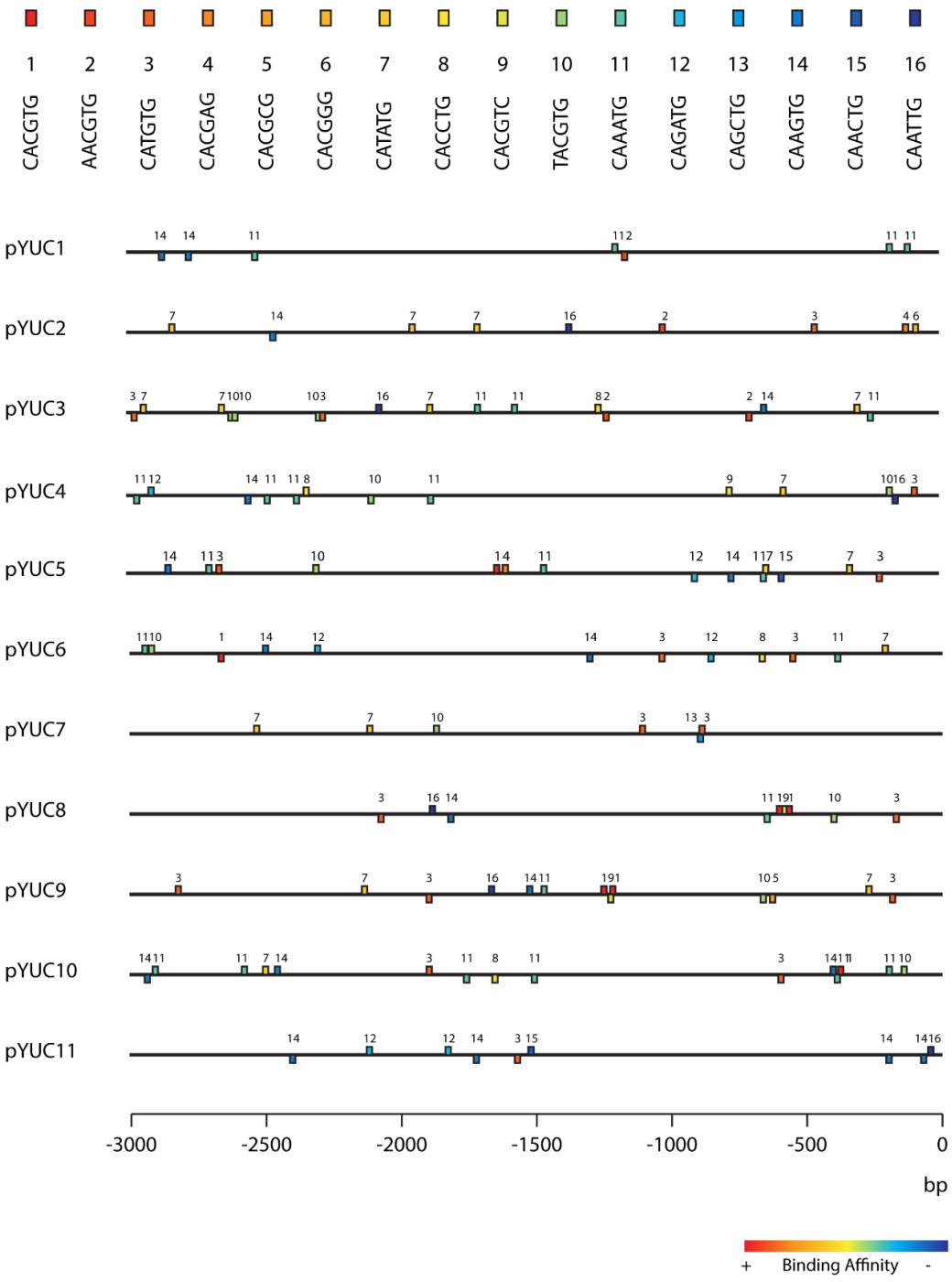


**Figure 3.** The promoter region of *YUC8* and *YUC9* presents a specific G-boxes binding motif configuration. Schematic representation of the distribution of *cis*-regulatory elements (G-box and G-box variants) in the promoter of *Arabidopsis YUCCA* genes. The conserved promoter region (from -3000 to -1) upstream to the transcriptional start point (ATG) of the eleven *YUCCA* family members is shown. All putative G-boxes are color-coded (square) and assigned with a specific sequence. Numbers indicate the corresponding G-box sequence, with number 1 being the canonical G-box. Different color indicates different experimental MYC2 binding affinities [32].

Preprints (www.preprints.org) | NOT PEER-REVIEWED | Posted: 6 July 2021 doi:10.20944/preprints202107.0142.v1

**MYC2 regulates *YUC8* and *YUC9* expression through the interaction with G-box elements**

We next studied whether the observed DNA binding sites are indeed involved in the transcriptional regulation of *YUC8* and *YUC9*. To this end we performed a transient transactivation effector-reporter experiment in *N. benthamiana* leaves. To prepare the effector plasmid, the independent *MYC2*, *MYC3* or *MYC4* open reading frames (ORFs) were isolated and fused to the *Cauliflower mosaic virus* (CaMV) 35S promoter to generate three constructs, *i.e. 35S::MYC2*, *35S::MYC3*, and *35S::MYC4* (Figure 4A). As reporter, a series of truncated promoter fragments from *YUC8* or *YUC9*, containing the tandem DNA motifs (191) or the final *cis*-acting element (#3), as well as a promoter segment containing none of these regulatory sequences (Ø), were amplified by PCR and cloned into a vector carrying the *ß-glucuronidase (GUS)* reporter gene. This resulted in the generation of three promoter constructs for pYUC8, *i.e. 191::GUS*, *3::GUS* and *Ø::GUS*, and three promoter constructs for *pYUC9*, *i.e. 191::GUS*, *3::GUS* and *Ø::GUS* (Figure 4A). Thereafter, we investigated GUS expression levels after *Agrobacterium tumefaciens*-mediated plant transformation (Figure 4B). Remarkably, the blue coloration demonstrated that the *GUS* expression, driven by the *191::GUS* and *3::GUS* constructs of both *YUC8* and *YUC9* promoters, was strongly activated in presence of either of the transcription factors MYC2, MYC3 or MYC4 relative to the fusion constructs *Ø::GUS*. Likewise, the detected weak blue staining perceived for the *Ø::GUS* constructs indicated a very weak background activity. In a second experiment, another group of agroinfiltrated leaf discs were utilized to quantify the transactivation of GUS reporter gene expression employing a fluorometric technique (Supplementary Figure A1). In agreement with the histochemical results we observed that the GUS activity of *191::GUS* and *3::GUS* samples increased 2-fold and 0.8-fold in pYUC8, and 2.3-fold and 1.3-fold in pYUC9, respectively in presence of MYC2. However, when the *N. benthamiana* leaves were co-infiltrated with different pYUC8 constructs and *35::MYC3*, the enzymatic analysis indicated that only the *191::GUS* construct was significantly activated, with almost 1.5-fold increase of the GUS activity compared to the negative control (empty vector). Interestingly, the absence of GUS activity in *3::GUS* may indicate that MYC3 does not effectively bind to the 5'-CATGTG-3' element #3. Nevertheless, the analysis of the *YUC9* promoter called this interpretation into question, since the fluorometric assay showed a strong activation of the GUS activity in *191::GUS* and *3::GUS* relative to the empty vector control (2.5-fold and 11.5-fold increased GUS activity, respectively). Finally, we detected that the transcription factor MYC4 significantly activated the *3::GUS* construct in the pYUC8, whereas in the pYUC9, both *191::GUS* and *3::GUS* showed 4.5-fold and 4-fold increased GUS activity levels, respectively, when compared to the negative control (Supplementary Figure A1). In contrast to MYC2 and MYC3, the presence of MYC4 only resulted in a moderate GUS activity for the *Ø::GUS* construct of pYUC8. This promoter fragment contains the G-box variant #11 (5'-CAAATG-3') in its sequence, suggesting that this *cis*-acting element could be important in the transcriptional regulation of *YUC8* exerted by MYC4. Overall, these analyses highlight MYC2 as the powerful positive regulator of both auxin biosynthetic genes, most probably through the interaction with the promoter G-box elements included in the "tandem" 1-9-1 (5'-CACGTG - CACGTC - CACGTG-3'), and/or the final *cis*-

Preprints (www.preprints.org) | NOT PEER-REVIEWED | Posted: 6 July 2021 doi:10.20944/preprints202107.0142.v1

regulatory G-box #3 (5'-CATGTG-3'). The results also suggest that MYC3 and MYC4 could act as possible co-operators in the transcriptional regulation of *YUC8* and *YUC9*.

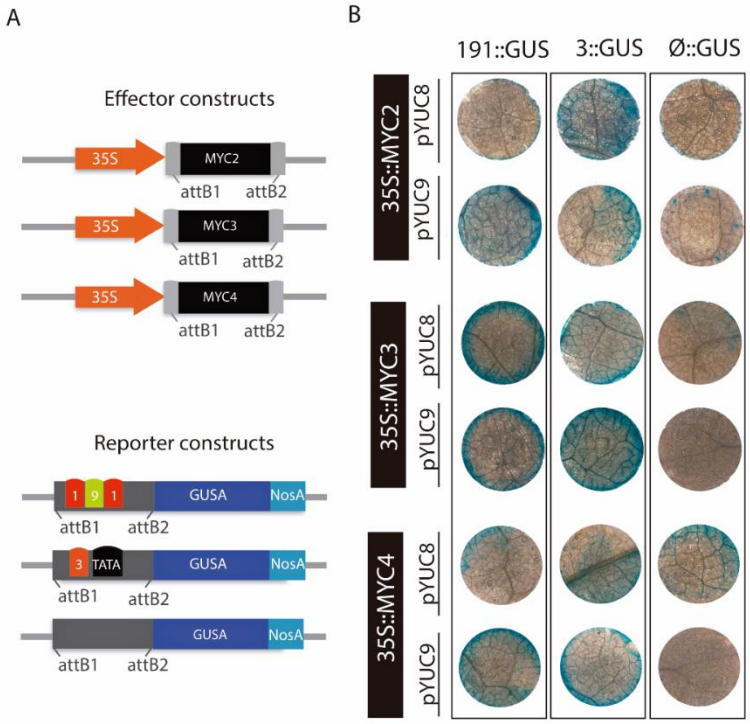


**Figure 4.** Transactivation of the *pYUC8::GUS* and *pYUC9::GUS* by MYC2, MYC3 and MYC4 proteins using agroinfiltrated *N. benthamiana* leaves. (**A**) Schematic representation of the effector and reporter constructs used in the transient expression experiment. The effector constructs contain the CaMV 35S promoter fused to the *MYC2*, *MYC3* and *MYC4* coding sequences. The reporter constructs contain different combinations of the G-box binding sites found in the YUC8/9 promoters, *i.e.*, the tandem 1-9-1 (5'-CACGTG - CACGTC - CACGTG-3'); the final *cis*-regulatory G-box #3 (5'-CATGTG-3'). Moreover, *Ø* refers to the promoter fragment lacking any of the mentioned DNA binding sites. All reporter constructs were fused to the *GUS* reporter gene, followed by the *Nos* terminator cassette. (**B**) Histochemical GUS staining of *N. benthamiana* leaf discs agroinfiltrated with the *191::GUS* and *3::GUS* constructs contain in the pYUC8/9 promoters in presence of the constitutively expressed MYC2, MYC3 and MYC4 transcription factors. The *Ø::GUS* construct was used as negative control.

To independently validate the interaction between MYC2 and YUC8/9 promoters by an alternative *in planta* method, we performed a third experiment in mesophyll protoplast of *A. thaliana* (Figure 5). Here, constructs analogous to those used for transient expression in *N. benthamiana* leaves were employed. They only differ in the plasmid backbone used for cloning. In addition, an empty pBT-10 vector was co-transfected with the *35::MYC2* effector constructs as negative control (Figure 5A). Confirming our previous findings, the relative values of GUS activity revealed that, in comparison to the negative control, the transcription factor MYC2 significantly activates the GUS reporter gene of the *191::GUS* and *3::GUS* constructs in both pYUC8 and pYUC9 (Figure 5B). Remarkably, the detected enzymatic GUS activity for the construct pYUC9-*Ø::GUS*, showed an increment of approximately 1.5-fold in comparison to the empty vector control. Like in the transactivation assay in *N. benthamiana*, this could be explained by the presence of the G-

Preprints (www.preprints.org) | NOT PEER-REVIEWED | Posted: 6 July 2021 doi:10.20944/preprints202107.0142.v1

box variants 5 (5'-CACGCG-3') and 10 (5'-TACGTG-3') in the promoter sequence used for these particular constructs. However, this conclusion is mainly based on the observation that no significant differences were found when compared to the negative control, which might be due to the high variability registered for the *Ø::GUS* samples. Most importantly, our results further support the notion that MYC2 directly binds to the G-box elements to promote *YUC8* and *YUC9* gene expression.

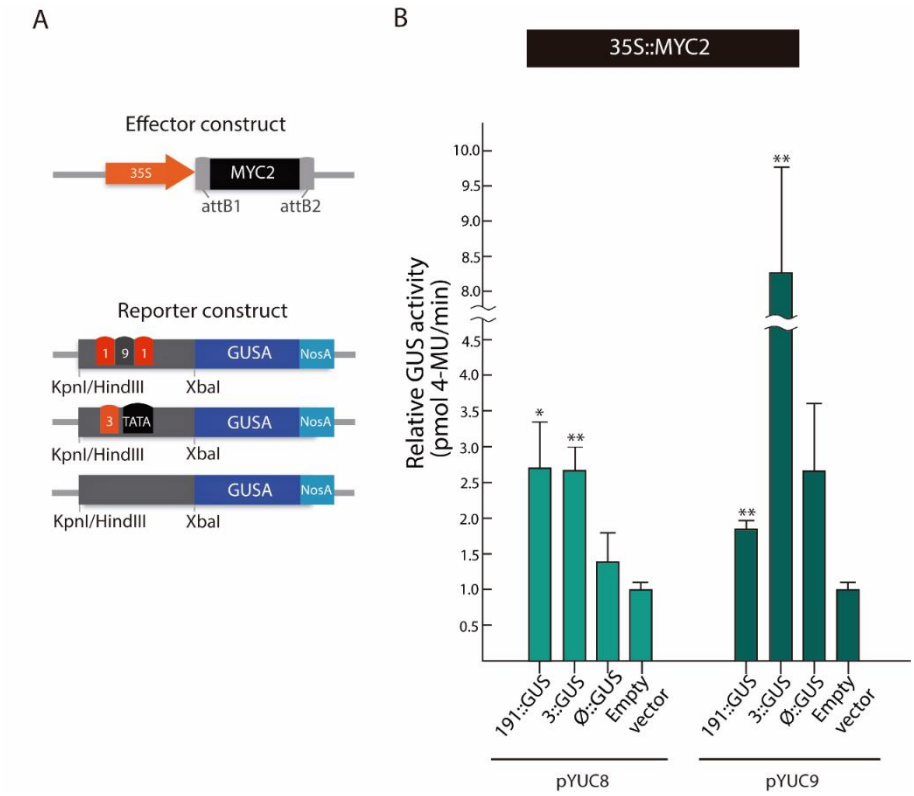


**Figure 5.** Transcriptional activity assay in *A. thaliana* mesophyll protoplasts. (**A**) Schematic representation of the effector constructs *35::MYC2* and the *191::GUS*, *3::GUS* and *Ø::GUS* reporter constructs used. (**B**) Fluorometric GUS activity quantification. The empty vector was used as negative control. The GUS activation levels were relativized to the *NAN* reporter gene activity and normalized to the empty vector. Final GUS activity levels are expressed as pmol 4-methylumelliferone (MU)/min. Values are mean ± SE. Three aliquots per protoplast suspension were analyzed. Similar results were obtained in two independent experiments. Asterisks indicate Student's *t*-test significant differences (*P < 0.05, **P < 0.01).

Preprints (www.preprints.org) | NOT PEER-REVIEWED | Posted: 6 July 2021 doi:10.20944/preprints202107.0142.v1

**YUC9 plays a role in biotic stress responses**

The bHLH transcription factor MYC2 plays a key role in JA-mediated defense response against herbivores and necrotrophic pathogens [23],[34-36]. This prompted us to investigate the activation of *YUC8* and *YUC9* expression by a phytophagous pest. To this end, 3 to 4 weeks-old wild-type plants and the reporter lines *pYUC8::GUS*, *pYUC9::GUS*, and *pAOS::GUS* were exposed to the two-spotted spider mite, *Tetranychus urticae*. Subsequent GUS staining clearly revealed a strong reporter activity for the positive control, the *AOS* (At5g42650) promoter line, and the *YUC9* promoter driven construct (Figure 6A). On the contrary, the absence of visible GUS activity in *pYUC8::GUS* leaves exposed to *T. urticae* suggests that *YUC8* is possibly not involve in the defense against pests or that the response of *YUC8* is slower than the response of *YUC9*, which has previously been suggested for oxylipin treatments (Hentrich *et al*., 2013a). In view of this result, we intended to shed light on the biological meaning of auxin synthesis driven by MYC2. Thus, WT, the overexpression line YUC9ox, and the *yuc9* knockout line (*yuc9ko*), were used to analyze as to whether alterations in *YUC9* expression has an influence on the susceptibility of plants toward herbivorous predators. To this end, ten adult female spider mites were placed on single leaves of ten plants for each genotype and allowed to feed for 4 days. The leaf damage quantification highlighted a preference of adult mites to feed on WT rather than YUC9ox plants. This is displayed by approximately 40% lower leaf damage area of YUC9ox compared to WT (Figure 6B). Interestingly, the *yuc9ko* mutants exhibited a decreased leaf damage area in comparison to WT, but the difference is statistically insignificant. Consistent with these observations, the DAB staining and the trypan blue exclusion test determined a visibly higher accumulation of reactive oxygen species (ROS) and cell death in WT and *yuc9ko* plants in comparison to YUC9ox (Supplementary Figure A2, Supplementary methods A2 and A3).

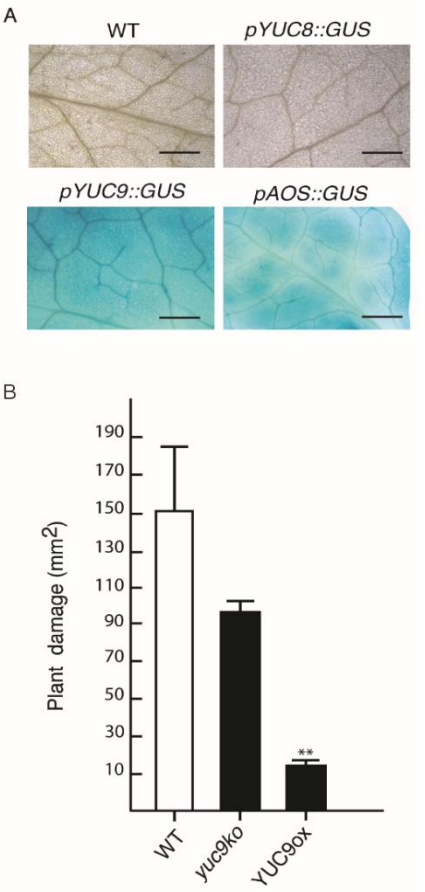


**Figure 6.** *YUC9* activation and plant damage assay after 4 days of spider mite (*Tetranychus urticae*) herbivory. (**A**) Histochemical GUS staining of leaves from wild-type *Arabidopsis*, *pYUC8::GUS*, *pYUC9::GUS* and *pAOS::GUS* plants, using 20 females from *T. urticae* per plant (n = 5). Scale bar = 50 µm. (**B**) Quantification of the total plant damage area (expressed in $mm^2$) in WT, *yuc9ko* and YUC9ox mutant lines. Represented are means ± SE (n = 5). Student's *t*-test: $^{**}P < 0.01$.

## 3. Discussion

The first indication of a positive JA-IAA crosstalk arouses from the observation that both

Preprints (www.preprints.org) | NOT PEER-REVIEWED | Posted: 6 July 2021 doi:10.20944/preprints202107.0142.v1

hormones share a conserved signal transduction mechanism that utilizes the 26S-proteosome system [37-39]. In line with this, during a mutant screening it became evident that a newly identified MeJA insensitive mutant was allelic to *axr1* defective mutant, which is impaired in auxin signaling [40], suggesting that AXR1 contributes to both, IAA and JA, perception. Likewise, it has been demonstrated that a point mutation in one subunit forming the SCF-E3 ligase complex of Arabidopsis resulted not only in reduced auxin response, but also in diminished expression of several JA-related genes [41]. In addition, it has been observed that JA and IAA cooperate spatiotemporally to regulate flower development and fertility trough the action of ARF6 and ARF8 [42]. In rice, the IAA-gradient generated during gravitropism is accompanied by a reciprocally oriented JA-gradient to co-regulate asymmetrical growth [43]. On the other hand, interconnectivity between JA signaling and IAA biosynthesis pathways have also been reported. Thus, two independent transcriptomic analysis revealed that among the group of up-regulated genes two *YUCCA* genes, *YUC8* and *YUC9*, were differentially induced by OPDA and MeJA [44, 45]. Meanwhile, Hentrich *et al*., (2013a) clearly demonstrated that wound-induced formation of MeJA in Col-0 Arabidopsis leaves is sufficient to trigger *YUC9* expression. Nevertheless, the molecular mechanism that controls *YUC8/9* expression remained uncertain.

In our effort to address whether these two auxin biosynthetic genes are direct downstream targets of the JA signaling pathway, we uncovered that MYC2, MYC3 and MYC4 are involve in *YUC8* and *YUC9* transcriptional regulation. Our GC-MS/MS and qRT-PCR experiments highlighted that JA-dependent IAA production driven by *YUC8* and *YUC9* is considerably dependent on the master JA regulator MYC2 (Figures 1-2). Likewise, we observed that MYC3 and MYC4 additionally contributed to auxin homeostasis, thereby confirming that these two transcription factors are phylogenetically closely related to MYC2 (Figure 1). We furthermore confirmed that MYC3 and MYC4 might also have a role in the transcriptional regulation of *YUC8* and *YUC9*, respectively. However, since we detected an induction of both genes in some loss-of-function mutants after MeJA treatment, the possibility that alternative regulatory elements also contribute to the translational control of *YUC8* and *YUC9* cannot be excluded (Figure 2A,B). Further extending this hypothesis, it is known that PIF4, which triggers hypocotyl elongation under high temperatures, can effectively bind to the G-motif located in the *YUC8* promoter [46]. Furthermore, the jasmonate inducible ETHYLENE RESPONSE FACTOR 109 (ERF109) has been reported to physically interact with the DNA-binding site 5′-GCCGCC-3′ to control *ASA1* and *YUC2* transcript accumulation [47]. Nevertheless, we did not identify the mentioned GCC-box motif in the promoter region of neither *YUC8* nor *YUC9*.

Here we demonstrated that all three described MYC proteins bind with similar, although not identical affinities to the core 5′-CACGTC-3′ motif, called G-box, and its variants [32], [48]. We analyzed the presence of these JA-responsive elements in the promoter sequence of the eleven Arabidopsis *YUCCA* members. Our results clearly identified a specific G-box motif configuration composed by the "tandem" 1-9-1 (5′- CACGTG-CACGTC-CACGTG-3′) followed by the G-box 3 (5′-CATGTG-3′) in the non-coding region of *YUC8* and *YUC9* (Figure 3). We provided multiple lines of supporting evidence, including

Preprints (www.preprints.org) | NOT PEER-REVIEWED | Posted: 6 July 2021 doi:10.20944/preprints202107.0142.v1

effector-reported assay in *N. benthamiana* and *A. thaliana* leaf protoplasts, to demonstrate that all three MYC transcription factors bind to the *YUC8* and *YUC9* promoters *in vivo*, when the 1-9-1 G-box-tandem or the 3 G-box variants are present (Figures 4, 5 and Supplementary Figure A1). Intriguingly, our experiments employing leaf protoplast further corroborated that MYC2 functions as a direct regulator of *YUC9* (Figure 5B).

Recently, Santamaría *et al.*, (2017) demonstrated that *T. urticae* infestation of Arabidopsis plants activates the MYC2 defense pathway. Taking advantage of this finding, we investigated the biological role of JA-induced IAA biosynthesis by performing a *T. urticae* feeding experiment. As shown in Figure 6A, the pest not only activated the *AOS* promoter, which is known to respond to wounding [50], but also the *YUC9* promoter. Recently, Zhurov *et al.*, (2014) reported the significant induction of JA production by *T. urticae* feeding in Arabidopsis Col-0 plants. Moreover, a more recent publication performed in *Nicotiana attenuate* showed the accumulation of auxin at the site of herbivory by *Manduca sexta* [52]. Intriguingly, this auxin accumulation was accompanied by a rapid activation of two YUCCA-like proteins. Thus, our results highlight the importance of the intimate crosstalk between JA and IAA through the modulation of *YUC9* expression in plant defense responses. Moreover, the *T. urticae* infestation experiments showed that the auxin overproducer line, YUC9ox, exhibited reduced plant-damage, $H_2O_2$ accumulation and cell death in comparison to similarly treated wild-type plants (Figure 6B and Supplementary Figure A2). It has been demonstrated that feeding of *T. urticae* on plant leaves proceeds via the insertion of their stylet between the pavement cells or through the open stoma [53]. Thus, it can be speculated that epidermal cell expansion is the cause of this enhanced tolerance by limiting spider mite feeding, rather than IAA-mediated immune activation. Congruent with this hypothesis, it has been observed that the transient overexpression of *YUC9* in *N. benthamiana* leaves resulted in significantly expanded pavement cells [27]. Alternatively, it is known that IAA and the biotic-stress related hormone ethylene, can interact at multiple levels [54]. For instance, earlier studies indicated that IAA stimulates ethylene production thought the action of specific *ACC-synthase* genes (ACS), which encode enzymes involved in a rate-limiting step of ethylene biosynthesis [55-59]. Likewise, Hentrich *et al.*, (2013b) reported up-regulation of several ethylene biosynthesis and signaling related genes in YUC8ox and YUC9ox lines. Therefore, we suggest that the JA-IAA-ET induced lignification contributes to complicate mite feeding or reduce palatability by increasing leaf rigidity and possibly reducing leaf nutritional values. The latter aspect is particularly supported by the observation that the spider mites actively left YUC9ox leaves, indicating that the spider mites detest feeding on those leaves.

## 4. Material and Methods

### Plant Material

In our study the *Arabidopsis thaliana* ecotype Columbia (Col-0) was used as wild type (WT). All different Arabidopsis *myc* mutants, *i.e.* single, double and triple T-DNA insertion lines *myc2*, *myc3*, *myc4*, *myc2myc3*, *myc2myc4*, *myc3myc4* and *myc2myc3myc4*, and the overexpression lines YUC9ox, as well as the T-DNA insertion mutant *yuc9ko* and the

Preprints (www.preprints.org) | NOT PEER-REVIEWED | Posted: 6 July 2021 doi:10.20944/preprints202107.0142.v1

reporter lines *pAOS::GUS*, *pYUC8::*GUS and *pYUC9::GUS* have been previously described elsewhere [27], [32], [50], [60]. Seeds were surface sterilized and sown on solidified ½-strength MS medium supplemented with 1% sucrose and stratified at 4 ºC for 48 h in darkness. Plant growth was performed under controlled conditions (22 °C, 16 h light/8 h dark and 100 µmol/m$^2$ s$^1$ light intensity). For plant defense experiments, we transferred 10-days old Arabidopsis plants to a mixture of peat and vermiculite (3:1) and we grew them under the same condition described above. The transactivation assay was carried out in 14-days old *N. benthamiana* seedlings transplanted to independent 13 cm diameter pots containing peat-based soil. Plants were grown under controlled greenhouse conditions (25 ºC and 40-65 % relative humidity) and a long-day photoperiod (16 h light/ 8 h dark) for 2 to 3 weeks.

**qRT-PCR analysis**

Here, we incubated 10-days old Arabidopsis seedlings with either 50 µM of MeJA or a control solution (0.5% methanol, v/v) over either 2 or 4 h, respectively [27]. Afterwards, total RNA was isolated using the phenol:chloroform method, coupled to lithium chloride precipitation, according to Box *et al*., (2011). Extracted RNA was reverse-transcribed into complementary DNA (cDNA) using the RNA-dependent DNA polymerase from Moloney-Murine Leukemia Virus (M-MLV) (Promega) following the manufactured instructions. Quantitative RT-PCRs were performed using a LightCycler® 480 (Roche) thermocycler following the manufacturer's instructions. For data accuracy, three independent biological replicates were tested in triplicates. The relative gene expression levels were calculated according the $2^{-\Delta\Delta Ct}$ method [62,63]. Primers used for analyzing mRNA levels are listed in Supplemental Table A1. *APT1* and *UBI10* were selected as the reference genes for data normalization [64].

**Auxin quantification**

Extraction of IAA was carried out according to Carrasco-Loba & Pollmann (2017). To this end, we harvested approximately 100 mg of 10 days-old seedlings in microcentrifuge tubes containing 1 ml of methanol and 50 pmol of the internal standard [$^2H_2$]-IAA (OlChemIm Ltd). After hormone extraction, IAA concentrations was examined by gas chromatography-mass spectrometry (GC-MS/MS). In brief, dried samples were resuspended in 20 µl of the freshly prepared derivatization solution [88 % acetone:methanol (9:1, v/v), 11.8 % diethyl ether, 1.2 % Trimethylsilyl diazomethane, 2 M in diethyl ether]. After incubation for 30 min at RT, 1 µl of the derivatized sample was injected splitless using a CLC CombiPal autosampler into a BRUKER Daltonics 451 gas chromatograph equipped with a stationary phase ZB-35 (30 m x 0.25 mm, 0.25 µm film) fused silica capillary column (Phenomenex). Helium at a flow rate of 1 ml min$^{-1}$ was used as the mobile phase for separation. The injector temperature was set to 250 ºC and the column was held at 50 ºC for 1.2 min, then temperature was increased by 30 ºC min$^{-1}$ to

Preprints (www.preprints.org) | NOT PEER-REVIEWED | Posted: 6 July 2021 doi:10.20944/preprints202107.0142.v1

120 ºC, and finally to 325 ºC by 10 ºC $min^{-1}$ and held there for 4 min more. The column effluent was introduced into the ion source of a Scion-TQ triple quadrupole mass spectrometer (BRUKER Daltonics). The transfer line and the ion source temperatures were maintained at 250 ºC and 200 ºC, respectively. Ions were generated by a 70 eV electron beam at an ionization current of 80 μA, and 30 spectra $s^{-1}$ were recorded in the mass range of 50 to 600 m/z. Under the given conditions the retention time for the endogenous methylated-IAA hormone was 13.6 min. For quantification, we selected the following precursor ions and corresponding diagnostic product ions; MeIAA (189/130) and [$^2H_2$]-MeIAA (191/132).

**_In silico_ analysis of _YUCCA_ promoter sequences**

Firstly, the full-length promoter sequences from the *A. thaliana YUC8* and *YUC9* genes were retrieved from the NCBI database (https://www.ncbi.nlm.nih.gov/gene/) and aligned using the online EMBOSS Matcher tool for pairwise sequence alignment. Following the determination of similarities in the promoter sequences, the predicted conserved regions obtained for the *A. thaliana YUC8* and *YUC9* promoter were used to identify and isolate the equivalent promoter sequences for the rest of the *A. thaliana YUCCA* family members. All different promoter sequences used in this work were retrieved from the NCBI gene database using the corresponding gene accession numbers: At4g32450 (*YUC1*), At4g13260 (*YUC2*), At1g04610 (*YUC3*), At5g11320 (*YUC4*), At5g43890 (*YUC5*), At5g25620 (*YUC6*), At2g33230 (*YUC7*), At4g28720 (*YUC8*), At1g04180 (*YUC9*), At1g48910 (*YUC10*), At1g21430 (*YUC11*). MYC2 binding motifs in the *YUC* promoter sequences were predicted by running target sequences against known *cis*-regulatory elements in the AtPan collection (http://atpan.itps.ncku.edu.tw/)[66] and PlantCare (http://bioinformatics.psb.ugent.be/webtools/plantcare/html/) [67] databases. To ensure the incorporation of all the possible G-box variants described by Fernández-Calvo *et al.* (2011) the promoter sequences were also manually inspected.

**Transient expression analysis in _Nicotiana benthamiana_**

The *YUC8* and *YUC9* promoter sequences, as well as the coding sequences from MYC2, MYC3 and MYC4 were amplified using PCR specific primers (Supplementary Table A1) and introduced into the entry vector pSP-Entry1 (Stephan Pollmann, not published). Subsequently, *pYUC8/9::GUS* and *35S::MYC2/3/4* constructs were obtained by transferring the target DNA fragments into the destination vectors pMDC-163 [68] or p35S-HA-GW [69,70] by LR reactions (Invitrogen). Then, we performed the *A. tumefaciens*-mediated transient expression as described in Ma *et al*., (2012). Briefly, Agrobacterium strain C58C1 carrying the desired construct and the Agrobacterium strain P19 carrying the suppressor of gene silencing from tomato bushy stunt virus (TBSV) were infiltrated into 3 to 4 weeks-old *N. benthamiana* plants. 3 days post inoculation, the infiltrated leaves were collected and the β-glucuronidase (GUS) activity was evaluated by histochemical analysis as detailed by Jefferson *et al*. (1987).

Preprints (www.preprints.org) | NOT PEER-REVIEWED | Posted: 6 July 2021 doi:10.20944/preprints202107.0142.v1

We also quantified GUS expression levels using a fluorometric analysis [73]. For this purpose, two leaf discs were frozen in liquid nitrogen ($N_2$), ground and re-suspended in 150 µl of GUS extraction solution [50 mM sodium phosphate buffer $Na_2HPO_4/NaH_2PO_4$ pH 7.5, 10 mM EDTA, 0.1 % (v/v) Triton X-100, 0.1 % (w/v) sodium lauroylsarcosinate (Sigma-Aldrich), 0.05 % (v/v) β-MeEtOH]. An aliquot of 10 µl was utilized for total protein content determination [74] using bovine-γ-globulin as the protein standard (Bio-Rad). Whereas an aliquot of 100 µl of the suspension was transferred to a 96-well clear flat bottom microtiter plate (Falcon) and mixed with 100 µl GUS extraction solution containing 4 mM of 4-methylumeliferyl-β-D-glucuronide (4-MUG) (Duchefa). Samples were then incubated at 37 ºC in the dark for 10 min ($T_0$). After the incubation, 100 µl the 4-MUG solution were transferred to a new 96-well plate and the reaction was stopped by the addition of 100 µl of 200 mM $Na_2CO_3$. The remaining sample (100 µl) was further incubated at 37 ºC in darkness for 1 h ($T_{60}$). Subsequently, fluorescence was measured at 360 nm excitation and 460 nm emission (56 gain, 10 flashes, 50 % mirror) using a TECAN Genios Pro fluorescence spectrometer (MTX Lab Systems). The GUS activity was calculated using the following equations:

$$GUS - Activity\ [pmol/min] = \frac{\Delta F/10}{t} \quad (1)$$

$$GUS\ Activity\ = \frac{GUS - Activity}{\text{mg of total protein}} \quad (2)$$

Where ΔF is the difference in fluorescence intensity $T_{60}$-$T_0$, 10 are the fluorescence units corresponding to 1 pmol of hydrolysed 4-MUG and $t$ is the time of incubation. Two independent experiments were carried out and GUS activity was quantified in triplicates to ensure accuracy.

**Arabidopsis protoplast-based transient expression**

To generate the reporter plasmids *pYUC8::GUS* and *pYUC9::GUS*, we amplified the promoter sequences of *YUC8* and *YUC9* containing different MYC2/3/4 binding sites, using PCR specific primers (Supplementary Table A1) and ligated into the pGEM®-T vector (Promega). Thereafter, DNA fragments were digested by restriction endonucleases and cloned into the PBT-10 plasmid [75]. On the other hand, the effector plasmids *35S:MYC2/3/4* were made as described above. In this case, however, pEarlyGate-210 [76] was used as destination vector. After construct generation, mesophyll protoplast isolation and PEG-calcium mediated DNA transfection were performed according to Mathur & Koncz (1998), Yoo *et al*. (2007), and Alonso *et al*. (2009). In this work, 9 µg of each reporter plasmid and 14 µg of the effector plasmid were utilized. Moreover, to normalize the transfection efficiency, 3 µg of the 35S::neuroaminidase (NAN) plasmid [73] were used. Then, GUS transactivation was quantified by fluorometric analysis as already described. Furthermore, NAN activity was determined according to Kirby & Kavanagh (2002). To do this, from the 150 µl resuspended protoplasts in GUS extraction solution a 10 µl aliquot

Preprints (www.preprints.org) | NOT PEER-REVIEWED | Posted: 6 July 2021 doi:10.20944/preprints202107.0142.v1

was mixed with 10 µl NAN extraction solution [50 mM $N_2HPO_4/NH_2PO_4$ pH 7.0, 10 mM EDTA, 0.1 % (v/v) Triton X-100, 0.1 % (w/v) sodium lauroylsarcosinate] containing freshly added 0.05 % (v/v) β-MeEtOH and 1 mM 2'-(4-methylumbelliferyl)-α-D-*N*-acetyl-neuroaminic acid (4-MUN) (Duchefa). The protoplasts were then incubated at 37 ºC in the dark for 10 min ($T_0$). After the incubation, 3.3 µl of the protoplast suspension was transferred to a 200 µl of NAN stop solution [330 mM $Na_2CO_3$]. The remaining protoplast/4-MUN solution was incubated at 37 ºC in darkness for 1 h ($T_{60}$). Afterwards, the fluorescence was measured as described before. NAN activity was calculated as [80]:

$$NAN - Activity\ [pmol/min] = \frac{\Delta F/10}{t} \quad (3)$$

Where ΔF is the difference in fluorescence $T_{60}$-$T_0$, 10 are the fluorescence units corresponding to 1 pmol of hydrolysed 4-MUN and $t$ is the time of incubation. Normalization of the GUS-activity was performed by calculating the ratio of GUS and NAN activities, represented as relative GUS/NAN units, following the equation:

$$\frac{GUS}{NAN} - Activity = \frac{GUS - Activity}{NAN - Activity} \quad (4)$$

To ensure data accuracy GUS and NAN activities were measured in triplicates and each experiment was repeated at least twice.

**Plant-arthropod interactions**

Adult female *T. urticae* spider mites, London strain, isolated from infested bean plants, were placed on leaves from 3 to 4-weeks-old *A. thaliana* plants according to Santamaria *et al*. (2017). The mites feed for four days in growth chambers (25 °C, 70% relative humidity and with a 16/8 h (light/dark) regime). Histochemical analyses of GUS activity were performed as described by Jefferson *et al*. (1987). For leaf damage quantification whole rosette of infested and control plants were scanned using a resolution of 1200 dpi. Plant damage was assessed as total area of chlorotic spots based on scanned leaves overlaid with a grid of 0.25 mm x 0.25 mm using Adobe Photoshop CS5 software (Adobe Systems, San Jose, CA) according to the following equation:

$$Area\ damage\ [mm^2] = number\ of\ dots\ x\ 0.25/0.25$$

Herein, the number of dots was calculated from the total number of pixels (derived from the histogram tool) divided by the number of pixels per dot (52 pixel/dot) [81]. We assessed plant damage was in five infested independent samples from each genotype.

**Statistics**

 doi:10.20944/preprints202107.0142.v1

The data were analyzed with Student's *t*-test when two means were compared. Statistical analyses were realized employing the STATGRAPHICS® Centurion XVI (Statpoint Technologies, INC.).

**Supplementary Materials:** The following are available online at www.mdpi.com/xxx/s1, **Figure A1.** Fluorometric quantification of GUS activity in *N. benthamiana* leaves agroinfiltrated with different YUC8 and YUC9 promoter fragments. **Figure A2.** Histochemical analysis after spider mite herbivory. **Methods A1.** Trypan Blue staining**. Methods A2.** DAB staining. **Table A1.** List of primers used for cloning and qRT-PCR analysis.

**Author Contributions:** S.P. and M.-M.P.-A. conceived and designed the research; M.-M.P.-A., B.S.-P., P.O.-G., M.E.S., I.D. and S.P. performed the research and analysed the data; S.P. was responsible for funding acquisition and wrote and edited the manuscript together with M.-M.P.-A.. All authors have read and agreed to the published version of the manuscript.

**Funding** This research was funded by the Spanish Ministry of Economy, Industry and Competitiveness (MINECO), grant number BFU2017-82826-R to S.P.

**Institutional Review Board Statement:** Not applicable.

**Informed Consent Statement:** Not applicable.

**Data Availability Statement:** All data supporting the findings of this study are available within the paper and within its supplementary data published online.

**Acknowledgments:** The authors thank Drs. Roberto Solano and Andrea Chini (Centro Nacional de Biotecnología, CNB-CSIC, Madrid) for kindly sharing the *myc* loss-of-function lines with us. In addition, the authors appreciate the thoughtful feedback and highly valuable comments by all members of the CBGP laboratories 127 and 132.

**Conflict of interest:** The authors declare no conflict of interests.

## Appendix A

**Methods A1.** Trypan Blue staining**.** Three to four weeks old infested *A. thaliana* leaves were harvested after 4 days of *T. urticae* feeding and stained with 5 ml lactophenol-trypan blue solution (10 ml lactic acid, 10 ml phenol, 10 ml glycerol, 10 ml tryptan blue (Sigma), dissolved in 10 ml of distilled $H_2O$) [1]. Before its use, the TB solution was diluted 1:2 with 100 % ethanol. The solution including two leaves was then boiled for 1 min and distained for 30 min at room temperature in 2 ml chloral hydrate solution (5 g of chloral hydrate dissolved in 2 ml distilled water). After overnight destaining, the chloral hydrate solution was removed and then 2 ml 50 % glycerol were added. Leaves were then placed on a microscope slide, covered with a cover slip and analyzed under bright-field lighting using a light stereomicroscope Leica MZ10F (Leica Microsystems) at a magnification of x8 and x40, respectively. Images were captured using a Leica DFC 400C camera (Leica Microsystems). Trypan blue staining was performed for five spider mite infested plants from each genotype and two control plants.

**Methods A2.** DAB staining. We examined $H_2O_2$ accumulation in three to four *A. thaliana* leaves exposed to 4 days of *T. urticae* feeding using the DAB staining method [2]. For this purpose, two leaves were placed in a 15 ml Falcon tubes, covered with 5 ml DAB solution (0.1 % (w/v) of 3,3-diaminobenzidine-HCl (pH 3,8)), vacuum infiltrated for 5 min and incubated overnight. After incubation, the DAB solution was supplemented with 10 mM ascorbic acid. Then, three subsequent washing steps with 5 ml ethanol/acetic acid/glycerol (v/v, 3:1:1) of 2 h each were performed to clear leaf tissues. Then 2 ml of 50% glycerol were added. Microscopy and imaging were carried out using a light stereomicroscope Leica MZ10F (Leica Microsystems), at a magnification of x8 and x40, and a Leica DFC 400C camera (Leica Microsystems). For this experiment were used, from each genotype, five spider mite infested plants and two control plants.

Preprints (www.preprints.org) | NOT PEER-REVIEWED | Posted: 6 July 2021 doi:10.20944/preprints202107.0142.v1

## Appendix A References

1 Koch, E.; Slusarenko, A., Arabidopsis Is Susceptible to Infection by a Downy Mildew Fungus. *Plant Cell* **1990**, *volume 2*, pp. 437–445, doi: 10.1105/tpc.2.5.437.

2 Thordal-Christensen, H.; Zhang, Z.; Wei, Y.; Collinge, D. B., Subcellular Localization of H2O2 in Plants. H2O2 Accumulation in Papillae and Hypersensitive Response during the Barley-Powdery Mildew Interaction. *Plant J.* **1997**, *volume 11*, pp. 1187–1194, doi: 10.1046/j.1365-313X.1997.11061187.x.

## Appendix B

**A1.** Fluorometric quantification of GUS activity in *N. benthamiana* leaves agroinfiltrated with different YUC8 and YUC9 promoter fragments. (**A**) Relative GUS activity of the 191::GUS, 3::GUS and *ø*::GUS reporter contructs co-transformed with the effector construct *35S::MYC2*, (**B**) *35S::MYC3*, and (**C**) *35S::MYC4*. In this case the empty pMDC163 vector was generated by the deletion of *ccdB* operon [1] and used as negative controlnegative control. GUS activity was then normalized according the empty vector and expressed as *p*mol 4-methylumelliferone (MU)/mg protein/min. Protein amunt was determined using Bradford method [2]. Data are mean ± SE. Three different leaves per plant were agroinfiltrated. The quantification of GUS activiry for wach promoter construct was measured in triplicates. Statistical analysis was perfomed using Student't t-test comparing between the negative contol and each promoter construct. Significan differencens between means are indicated with asterisks (*P < 0.05, **P < 0.01).

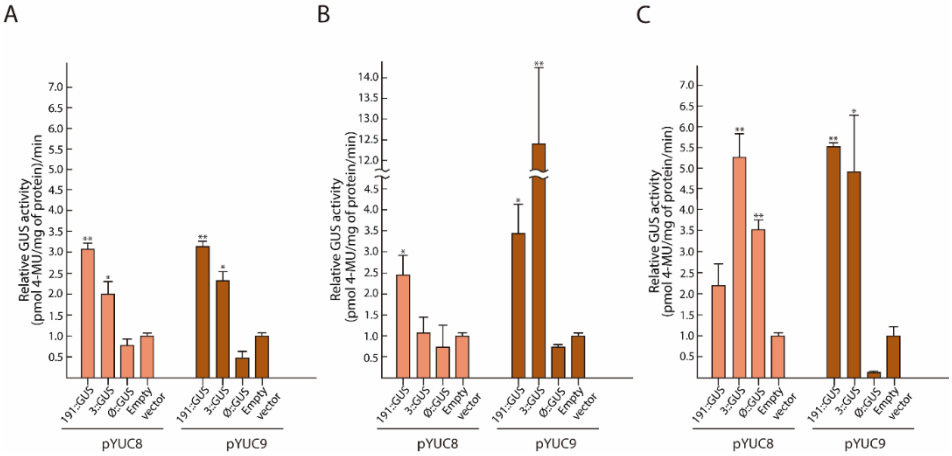


**A2.** Histochemical analysis after spider mite herbivory. (**A**) DAB staining, (**B**) Trypan blue staining. Arrows indicate $H_2O_2$ accumulation and cell death, respectively. Images represent leaf details of control plants (top row) and plants exposed to 4 days spider mite feeding (bottom row). Scale bar = 1 mm.

Preprints (www.preprints.org) | NOT PEER-REVIEWED | Posted: 6 July 2021 doi:10.20944/preprints202107.0142.v1

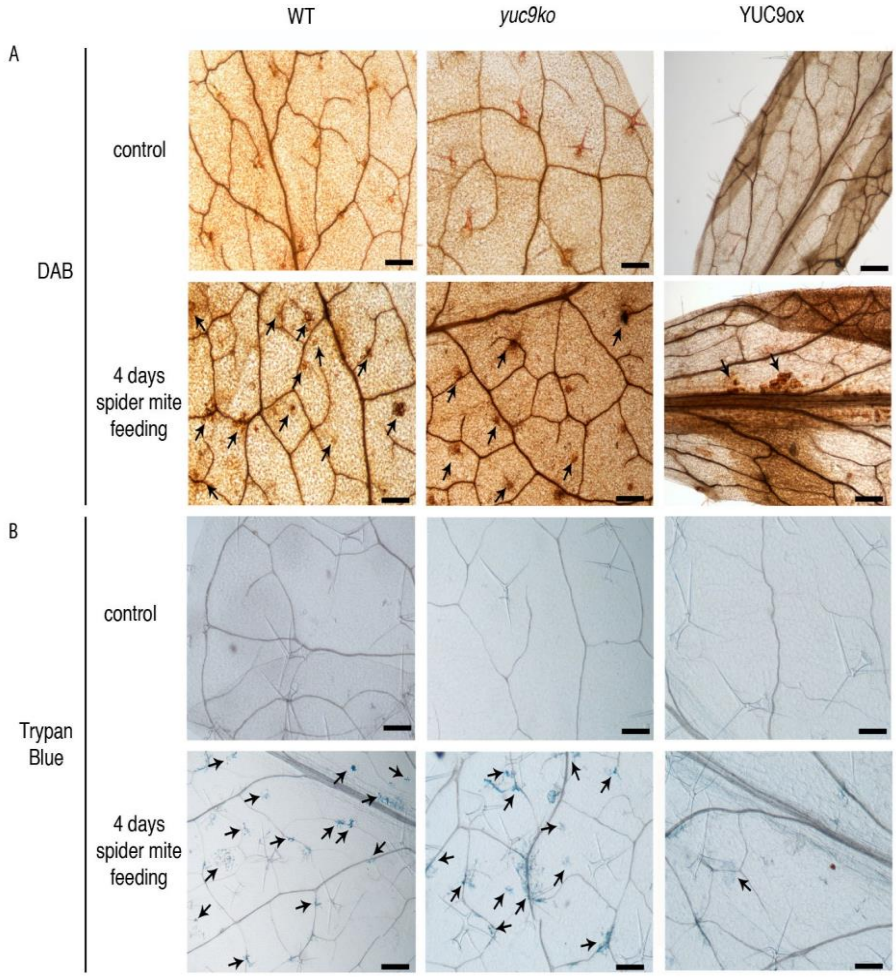


**Table S1.** List of primers used for cloning and qRT-PCR analysis (www.quantprimer.de) [3]

| Primer Name | Primer sequence (5′-3′) and restriction sites |
|---|---|
| Promoter YUC8-(919) For | TATGGATCCAAAAGTGCAGCGTCTACCAAAA |
| Promoter YUC8-(919) Rev | TATTCTAGATTAGGTACGGAAAATGTGATT |
| Promoter YUC8-(3) For | TATGGATCCTCCGTACCTAAAAATTGGATT |
| Promoter YUC8-(3) Rev | TATTCTAGATGCTTGACGACGAAGTAATAAT |
| Promoter YUC8-(Ø) For | TATGGATCCTCGTCGTCAAGCATTATCACTGTT |
| Promoter YUC8-(Ø) Rev | TATCCATGGTCTAGATGGAAGTTGTATTGGAAATGGTTT |
| Promoter YUC9-(919) For | TATAAGCTTAACAAAATTAGGACCCGCTCT |
| Promoter YUC9-(919) Rev | TATTCTAGAGATTGAATTATATGGTAAACTCAA |
| Promoter YUC9-(3) For | TATAAGCTTACCACGAAGAAAATAACATCTC |
| Promoter YUC9-(3) Rev | TATCCATGGTCTAGAGTTAAGAGTTATAACGAGACTG |
| Promoter YUC9-(Ø) For | TATAAGCTTCAAATTATTCACATTAATAAAATAATC |
| Promoter YUC9-(Ø) Rev | TATCCATGGTCTAGATTTCTTGAGTGAGTTTTTGAATG |
| ORF MYC2 For | TATGGTACCATGACTGATTACCGGCTACAACCAACGA |
| ORF MYC2 Rev | TATGCGGCCGCTTAACCGATTTTTGAAATCAAACTTGCTCTGA |
| ORF MYC3 For | TATGGATCCATGAACGGCACAACATCATCA |
| ORF MYC3 Rev | TATGATATCTCAATAGTTTTCTCCGACTTTCGT |
| ORF MYC4 For | TATGGATCCATGTCTCCGACGAATGTTCAAGTAACCGA |
| ORF MYC4 Rev | TATGATATCTCATGGACATTCTCCAACTTTCTCCGTT |

| | |
|---|---|
| pENTRY-SP1 For | TATCTGATAGTGACCTGTTCGTTGCA |
| pENTRY-SP1 Rev | TATGGAGATCCGTGACGCAGTAGC |
| pBT-10-Seq Rev | TATTTGGGGTTTCTACAGGACGGACCAT |
| pENTRY-SP1 Rev | TATGGAGATCCGTGACGCAGTAGC |
| YUC8-qPCR For | CGTCTCAAGCTTCACCTTCC |
| YUC8-qPCR Rev | AGCCACTGGTCTCATCGAAC |
| YUC9-qPCR For | TTCTCGCCACCGGTTATCGTAG |
| YUC9-qPCR Rev | AGCGATGTTAACGGCGTCTACTG |
| APT1-qPCR For | TCGTGCTGTTCCTTGCAACCG |
| APT1-qPCR Rev | GCGGAGGAGAAGAGGCGGAGT |
| UBI10-qPCR For | TTGGAGGATGGCAGAACTCTTGCT |
| UBI10-qPCR Rev | AGTTTTCCCAGTCAACGTCTTAACGAAA |

## AppendixB references


1 Miki, T.; Ae Park, J.; Nagao, K.; Murayama, N.; Horiuchi, T., Control of Segregation of Chromosomal DNA by Sex Factor F in Escherichia Coli. Mutants of DNA Gyrase Subunit A Suppress LetD (CcdB) Product Growth Inhibition. *J. Mol. Biol.* **1992**, *volume 225*, pp. 39–52, doi: 10.1016/0022-2836(92)91024-J.

2 Bradford, M. M., A Rapid and Sensitive Method for the Quantitation of Microgram Quantities of Protein Utilizing the Principle of Protein-Dye Binding. *Anal. Biochem.* **1976**, *volume 72*, pp. 248–254, doi: 10.1016/0003-2697(76)90527-3.

3 Arvidsson, S.; Kwasniewski, M.; Riano-Pachon, D. M.; Mueller-Roeber, B., QuantPrime - a Flexible Tool for Reliable High-Throughput Primer Design for Quantitative PCR. *BMC Bioinformatics* **2008**, *volume 9*, p. 465, doi: 10.1186/1471-2105-9-465.


## References


1 Kögl, F.; Erxleben, H.; Haagen-Smit, A. J., Über Die Isolierung Der Auxine a Und b Aus Pflanzlichen Materialien. 9. Mitteilung Über Pflanzliche Wachstumsstoffe. *Hoppe-Seyler's Zeitschrift für physiologishe Chemie* **1934**, *volume 225*, pp. 215–229, doi: doi:10.1515/bchm2.1934.225.5-6.215.

2 Thimann, K. V; Koepfli, J. B., Identity of the Growth-Promoting and Root-Forming Substances of Plants. *Nature* **1935**,*volume 135*, pp. 101–102, doi: 10.1038/135101a0.

3 Went, F. W., Auxin, the Plant Growth-Hormone. *Bot. Rev.* **1935**, *volume 1*, pp. 162–182, doi: 10.1007/BF02870150.

4 Woodward, A. W.; Bartel, B., Auxin: Regulation, Action, and Interaction. *Ann. Bot.* **2005**, *volume 95*, pp. 707–735, doi: 10.1093/aob/mci083.

5 Paponov, I. A.; Paponov, M.; Teale, W.; Menges, M.; Chakrabortee, S.; *et al.*, Comprehensive Transcriptome Analysis of Auxin Responses in Arabidopsis. *Mol. Plant* **2008**, *volume 1*, pp. 321–337, doi: 10.1093/mp/ssm021.

6 Abel, S.; Theologis, A., Odyssey of Auxin. *Cold Spring Harb. Perspect. Biol.* **2010**, *volume 2*, pp. 1–13, doi: 10.1101/cshperspect.a004572.

7 McGuire, R.; Agrawal, A. A., Trade-Offs between the Shade-Avoidance Response and Plant Resistance to Herbivores? Tests with Mutant Cucumis Sativus. *Funct. Ecol.* **2005**, *volume 19*, pp. 1025–1031, doi: 10.1111/j.1365-2435.2005.01047.x.

8 Walters, D.; Heil, M., Costs and Trade-Offs Associated with Induced Resistance. *Physiol. Mol. Plant Pathol.* **2007**, *volume 71*, pp. 3–17, doi: 10.1016/j.pmpp.2007.09.008.

9 Kempel, A.; Schädler, M.; Chrobock, T.; Fischer, M.; van Kleunen, M., Tradeoffs Associated with Constitutive and Induced Plant Resistance against Herbivory. *Proc. Natl. Acad. Sci. U. S. A.* **2011**, *volume 108*, pp. 5685–5689, doi: 10.1073/pnas.1016508108.

10 Leone, M.; Keller, M. M.; Cerrudo, I.; Ballaré, C. L., To Grow or Defend? Low Red: Far-Red Ratios Reduce Jasmonate Sensitivity in Arabidopsis Seedlings by Promoting DELLA Degradation and Increasing JAZ10 Stability. *New Phytol.* **2014**, *volume 204*, pp. 355–367, doi: 10.1111/nph.12971.

11 Huot, B.; Yao, J.; Montgomery, B. L.; He, S. Y., Growth-Defense Tradeoffs in Plants: A Balancing Act to Optimize Fitness. *Mol. Plant* **2014**, *volume 7*, pp. 1267–1287, doi: 10.1093/mp/ssu049.

12 Kurashige, N. S.; Agrawal, A. A., Phenotypic Plasticity to Light Competition and Herbivory in *Chenopodium Album* (Chenopodiaceae). *Am. J. Bot.* **2005**, *volume 92*, pp. 21–26, doi: 10.3732/ajb.92.1.21.

13 Griebel, T.; Zeier, J., Light Regulation and Daytime Dependency of Inducible Plant Defenses in Arabidopsis: Phytochrome Signaling Controls Systemic Acquired Resistance Rather than Local Defense. *Plant Physiol.* **2008**, *volume 147*, pp. 790–801, doi: 10.1104/pp.108.119503.

14 Mutka, A. M.; Fawley, S.; Tsao, T.; Kunkel, B. N.; Louis, S., Auxin Promotes Susceptibility to *Pseudomonas Syringae* via a Mechanism Independent of Suppression of Salicylic Acid-Mediated Defenses. *Plant J.* **2013**, pp. 746–754, doi: 10.1111/tpj.12157.

15 Fahlgren, N. *et al.*, Regulation of AUXIN RESPONSE FACTOR3 by TAS3 Ta-SiRNA Affects Developmental Timing and Patterning in Arabidopsis. *Curr. Biol.* **2006**, *volume 16*, pp. 939–944, doi: 10.1016/j.cub.2006.03.065.

16 Zhang, T. *et al.*, Hormone Crosstalk in Wound Stress Response: Wound-Inducible Amidohydrolases Can Simultaneously Regulate Jasmonate and Auxin Homeostasis in Arabidopsis Thaliana. *J. Exp. Bot.* **2016**, *volume 67*, pp. 2107–2120, doi: 10.1093/jxb/erv521.

17 Sweeney, C.; Lakshmanan, V.; Bais, H. P., Interplant Aboveground Signaling Prompts Upregulation of Auxin Promoter and Malate Transporter as Part of Defensive Response in the Neighboring Plants. *Front. Plant Sci.* **2017**, *volume 8*,. pp 1-10. doi: 10.3389/fpls.2017.00595

18 Böttcher, C.; Pollmann, S., Plant Oxylipins: Plant Responses to 12-Oxo-Phytodienoic Acid Are Governed by Its Specific Structural and Functional Properties. *FEBS J.* **2009**, *volume 276*, pp. 4693–4704, doi: 10.1111/j.1742-4658.2009.07195.x.

19 Koo, A. J. K.; Howe, G. A., The Wound Hormone Jasmonate. *Phytochemistry* **2009**, *volume 70*, pp. 1571–1580, doi: 10.1016/j.phytochem.2009.07.018.

20 Wasternack, C.; Forner, S.; Strnad, M.; Hause, B., Jasmonates in Flower and Seed Development. *Biochimie* **2013**, *volume 95*, pp. 79–85, doi: 10.1016/j.biochi.2012.06.005.

21 Pérez-Alonso, MM.; Pollmann, S., How Auxin May Contribute to the Regulation of Plant Defense Responses against Herbivory. *Austin J. Plant Biol.* **2018**, *volume 4*, pp. 1–5, doi: 10.26420/austinjplantbiol.2018.1019.

22 Chini, A.; Fonseca, S.; Fernández, G.; Adie, B.; Chico, J. M.; *et al.*, The JAZ Family of Repressors Is the Missing Link in Jasmonate Signalling. *Nature* **2007**, *volume 448*, pp. 666–671, doi: 10.1038/nature06006.

23 Kazan, K.; Manners, J. M., MYC2: The Master in Action. *Mol. Plant* **2013**, *volume 6*, pp. 686–703, doi: https://doi.org/10.1093/mp/sss128.

24 Chen, Q.; Sun, J.; Zhai, Q.; Zhou, W.; Qi, L.; *et al.*, The Basic Helix-Loop-Helix Transcription Factor MYC2 Directly Represses *PLETHORA* Expression during Jasmonate-Mediated Modulation of the Root Stem Cell Niche in Arabidopsis. *Plant Cell***.** **2011**, *volume 23*, pp. 3335 LP – 3352, doi: 10.1105/tpc.111.089870.

25 Dombrecht, B.; Xue, G. P.; Sprague, S. J.; Kirkegaard, J. A.; Ross, J. J.; *et al.*, MYC2 Differentially Modulates Diverse Jasmonate-Dependent Functions in Arabidopsis. *Plant Cell* **2007**, *volume 19*, pp. 2225–2245, doi: 10.1105/tpc.106.048017.

26 Sun, J.; Xu, Y.; Ye, S.; Jiang, H.; Chen, Q.; *et al.*, Arabidopsis ASA1 Is Important for Jasmonate-Mediated Regulation of Auxin Biosynthesis and Transport during Lateral Root Formation. *Plant Cell* **2009**, *volume 21*, pp. 1495–511, doi: 10.1105/tpc.108.064303.

27 Hentrich, M.; Böttcher, C.; Düchting, P.; Cheng, Y.; Zhao, Y.; *et al.*, The Jasmonic Acid Signaling Pathway Is Linked to Auxin Homeostasis through the Modulation of *YUCCA8* and *YUCCA9* Gene Expression. *Plant J.* **2013a**, *volume 74*, pp. 626–637, doi: 10.1111/tpj.12152.

28 Cheng, Y.; Dai, X.; Zhao, Y., Auxin Synthesized by the YUCCA Flavin Monooxygenases Is Essential for Embryogenesis and Leaf Formation in Arabidopsis. *Plant Cell* **2007**, *volume 19*, pp. 2430–9, doi: 10.1105/tpc.107.053009.

29 Stepanova, A. N.; Robertson-Hoyt, J.; Yun, J.; Benavente, L. M.; Xie, D.-Y.; *et al.*, TAA1-Mediated Auxin Biosynthesis Is Essential for Hormone Crosstalk and Plant Development. *Cell* **2008**, *volume 133*, pp. 177–191, doi: 10.1016/j.cell.2008.01.047.

30 Won, C.; Shen, X.; Mashiguchi, K.; Zheng, Z.; Dai, X.; *et al.*, Conversion of Tryptophan to Indole-3-Acetic Acid by TRYPTOPHAN AMINOTRANSFERASES OF ARABIDOPSIS and YUCCAs in Arabidopsis. *Proc. Natl. Acad. Sci.* **2011**, *volume 108*, pp. 18518–18523, doi: 10.1073/pnas.1108436108.

31 Mano, Y.; Nemoto, K., The Pathway of Auxin Biosynthesis in Plants. *J. Exp. Bot.* **2012**, *volume 63*, pp. 2853–2872, doi: 10.1093/jxb/ers091.

32 Fernández-Calvo, P.; Chini, A.; Fernández-Barbero, G.; Chico, J.-M.; Gimenez-Ibanez, S.; *et al.*, The Arabidopsis BHLH Transcription Factors MYC3 and MYC4 Are Targets of JAZ Repressors and Act Additively with MYC2 in the Activation of Jasmonate Responses. *Plant Cell* **2011**, *volume 23*, pp. 701–715, doi: 10.1105/tpc.110.080788.

33 Kiran, K. *et al.*, The TATA-Box Sequence in the Basal Promoter Contributes to Determining Light-Dependent Gene Expression in Plants. *Plant Physiol.* **2006**, *volume 142*, pp. 364–76, doi: 10.1104/pp.106.084319.

34 Turner, J. G.; Ellis, C.; Devoto, A., The Jasmonate Signal Pathway. *Plant Cell* **2002**, *volume 14*, pp. S153-64, doi: 10.1105/tpc.000679.

35 Lorenzo, O.; Chico, J. M.; Sánchez-Serrano, J. J.; Solano, R., JASMONATE-INSENSITIVE1 Encodes a MYC Transcription Factor Essential to Discriminate between Different Jasmonate-Regulated Defense Responses in Arabidopsis. *Plant Cell* **2004**, *volume 16*, pp. 1938–1950, doi: 10.1105/tpc.022319.

36 Schweizer, F.; Fernández-Calvo, P.; Zander, M.; Diez-Diaz, M.; Fonseca, S.; *et al.*, Arabidopsis Basic Helix-Loop-Helix Transcription Factors MYC2, MYC3, and MYC4 Regulate Glucosinolate Biosynthesis, Insect Performance, and Feeding Behavior. *Plant Cell* **2013**, *volume 25*, pp. 3117–32, doi: 10.1105/tpc.113.115139.

37 Hoffmann, M.; Hentrich, M.; Pollmann, S., Auxin-Oxylipin Crosstalk: Relationship of Antagonists. *J. Integr. Plant Biol.* **2011**, *volume 53*, pp. 429–445, doi: 10.1111/j.1744-7909.2011.01053.x.

38 Pérez, A. C.; Goossens, A., Jasmonate Signalling: A Copycat of Auxin Signalling?. *Plant, Cell Environ.* **2013**, *volume 36*, pp. 2071–2084, doi: 10.1111/pce.12121.

39 Shabek, N.; Zheng, N., Plant Ubiquitin Ligases as Signaling Hubs. *Nat. Struct. Mol. Biol.* **2014**, *volume 21*, pp. 293–296, doi: 10.1038/nsmb.2804.

40 Tiryaki, I.; Staswick, P. E., An Arabidopsis Mutant Defective in Jasmonate Response Is Allelic to the Auxin-Signaling Mutant Axr1. *Plant Physiol.* **2002**, *volume 130*, pp. 887–894, doi: 10.1104/pp.005272.

41 Ren, C.; Pan, J.; Peng, W.; Genschik, P.; Hobbie, L.; *et al.*, Point Mutations in Arabidopsis Cullin1 Reveal Its Essential Role in Jasmonate Response. *Plant J.* **2005**, *volume 42*, pp. 514–524, doi: 10.1111/j.1365-313X.2005.02394.x.

42 Nagpal, P.; Ellis, C. M.; Weber, H.; Ploense, S. E.; Barkawi, L. S.; *et al.*, Auxin Response Factors ARF6 and ARF8 Promote Jasmonic Acid Production and Flower Maturation. *Development* **2005**, *volume 132*, pp. 4107–4118, doi: 10.1242/dev.01955.

43 Gutjahr, C.; Riemann, M.; Müller, A.; Düchting, P.; Weiler, E. W.; Nick, P., Cholodny-Went Revisited: A Role for Jasmonate in Gravitropism of Rice Coleoptiles. *Planta* **2005**, *volume 222*, pp. 575–585, doi: 10.1007/s00425-005-0001-6.

44 Mueller, S.; Hilbert, B.; Dueckershoff, K.; Roitsch, T.; Krischke, M.; *et al.*, General Detoxification and Stress Responses Are Mediated by Oxidized Lipids through TGA Transcription Factors in Arabidopsis. *Plant Cell* **2008**, *volume 20*, pp. 768–785, doi: 10.1105/tpc.107.054809.

45 Pauwels, L.; Morreel, K.; De Witte, E.; Lammertyn, F.; Van Montagu, M.; *et al.*, Mapping Methyl Jasmonate-Mediated Transcriptional Reprogramming of Metabolism and Cell Cycle Progression in Cultured Arabidopsis Cells. *Proc Natl Acad Sci USA* **2008**, *volume 105*, pp. 1380–1385, doi: 0711203105 [pii]\r10.1073/pnas.0711203105.

46 Sun, J.; Qi, L.; Li, Y.; Chu, J.; Li, C., PIF4-Mediated Activation of *YUCCA8* Expression Integrates Temperature into the Auxin Pathway in Regulating Arabidopsis Hypocotyl Growth. *PLoS Genet.* **2012**, *volume 8*, p. e1002594, doi: 10.1371/journal.pgen.1002594.

47 Cai, X.-T.; Xu, P.; Zhao, P.-X.; Liu, R.; Yu, L.-H.; Xiang, C.-B., Arabidopsis ERF109 Mediates Cross-Talk between Jasmonic Acid and Auxin Biosynthesis during Lateral Root Formation. *Nat. Commun.* **2014**, *volume 5*, p. 5833, doi: 10.1038/ncomms6833.

48 Chini, A.; Boter, M.; Solano, R., Plant Oxylipins: COI1/JAZs/MYC2 as the Core Jasmonic Acid-Signalling Module. *FEBS J.* **2009**,

*volume 276*, pp. 4682–4692, doi: 10.1111/j.1742-4658.2009.07194.x.

49 Santamaría, M. E.; Martinez, M.; Arnaiz, A.; Ortego, F.; Grbic, V.; Diaz, I., MATI, a Novel Protein Involved in the Regulation of Herbivore-Associated Signaling Pathways. , *Front. Plant Sci.*, **2017**, *volume 8*,. p. 975, 2017. doi: 10.3389/fpls.2017.00975

50 Kubigsteltig, I.; Laudert, D.; Weiler, E. W., Structure and Regulation of the Arabidopsis Thaliana Allene Oxide Synthase Gene. *Planta* **Jun. 1999**, *volume 208*, pp. 463–471, doi: 10.1007/s004250050583.

51 Zhurov, V.; Navarro, M.; Bruinsma, K. A.; Arbona, V.; Santamaria, M. E.; *et al.*, Reciprocal Responses in the Interaction between Arabidopsis and the Cell-Content-Feeding Chelicerate Herbivore Spider Mite. *Plant Physiol.* **2014**, *volume 164*, pp. 384–399, doi: 10.1104/pp.113.231555.

52 Machado, R. A. R.; Robert, C. A. M.; Arce, C. C. M.; Ferrieri, A. P.; Xu, S.; *et al.*, Auxin Is Rapidly Induced by Herbivore Attack and Regulates a Subset of Systemic, Jasmonate-Dependent Defenses. *Plant Physiol.* **2016**, *volume 172*, pp. 521–532, doi: 10.1104/pp.16.00940.

53 Bensoussan, N.; Santamaria, M. E.; Zhurov, V.; Diaz, I.; Grbic, M.; Grbic, V., Plant-Herbivore Interaction: Dissection of the Cellular Pattern of *Tetranychus Urticae* Feeding on the Host Plant. *Front. Plant Sci.* **2016**, *volume 7*, p. 1105, doi: 10.3389/FPLS.2016.01105.

54 Stepanova, A. N.; Yun, J.; Likhacheva, A. V.; Alonso, J. M., Multilevel Interactions between Ethylene and Auxin in Arabidopsis Roots. *Plant Cell Online* **2007**, *volume 19*, pp. 2169–2185, doi: 10.1105/tpc.107.052068.

55 Jones, J. F.; Kende, H., Auxin-Induced Ethylene Biosynthesis in Subapical Stem Sections of Etiolated Seedlings of Pisum Sativum L. *Planta* **1979**, *volume 146*, pp. 649–56, doi: 10.1007/BF00388846.

56 Yu, Y. B.; Adams, D. O.; Yang, S. F., Regulation of Auxin-Induced Ethylene Production in Mung Bean Hypocotyls: Role of 1-Aminocyclopropane-1-Carboxylic Acid. *Plant Physiol.* **1979**, *volume 63*, pp. 589–90, doi: 10.1104/PP.63.3.589.

57 Yang, S. F.; Hoffman, N. E., Ethylene Biosynthesis and Its Regulation in Higher Plants. *Annu. Rev. Plant Physiol.* **1984**, *volume 35*, pp. 155–189, doi: 10.1146/annurev.pp.35.060184.001103.

58 Abel, S.; Nguyen, M. D.; Chow, W.; Theologis, A., *ASC4*, a Primary Indoleacetic Acid-Responsive Gene Encoding 1-Aminocyclopropane-1-Carboxylate Synthase in Arabidopsis Thaliana: Structural Characterization, Expression in Escherichia Coli, and Expression Characteristics in Response to Auxin. *J. Biol. Chem.* **1995**, *volume 270*, pp. 19093–19099, doi: 10.1074/jbc.270.32.19093.

59 Tsuchisaka, A.; Yu, G.; Jin, H.; Alonso, J. M.; Ecker, J. R.; *et al.*, A Combinatorial Interplay among the 1-Aminocyclopropane-1-Carboxylate Isoforms Regulates Ethylene Biosynthesis in Arabidopsis Thaliana. *Genetics* **2009**, *volume 183*, pp. 979–1003, doi: 10.1534/genetics.109.107102.

60 Hentrich, M.; Sánchez-Parra, B.; Pérez Alonso, M.-M.; Carrasco Loba, V.; Carrillo, L.; *et al.*, YUCCA8 and YUCCA9 Overexpression Reveals a Link between Auxin Signaling and Lignification through the Induction of Ethylene Biosynthesis. *Plant Signal. Behav.* **2013b**, *volume 8*, e26363-1, doi: 10.4161/psb.26363.

61 Box, M. S.; Coustham, V.; Dean, C.; Mylne, J. S., Protocol: A Simple Phenol-Based Method for 96-Well Extraction of High Quality RNA from Arabidopsis. *Plant Methods* **2011**, *volume 7*, p. 1-10, doi: 10.1186/1746-4811-7-7.

62 Livak, K. J.; Schmittgen, T. D., Analysis of Relative Gene Expression Data Using Real-Time Quantitative PCR and the 2−ΔΔCT Method. *Methods* **2001**, *volume 25*, pp. 402–408, doi: 10.1006/meth.2001.1262.

63 Schmittgen, T. D.; Livak, K. J., Analyzing Real-Time PCR Data by the Comparative CT Method. *Nat. Protoc.* **2008**, *volume 3*, pp. 1101–1108, doi: 10.1038/nprot.2008.73.

64 Czechowski, T.; Stitt, M.; Altmann, T.; Udvardi, M. K.; Scheible, W.-R., Genome-Wide Identification and Testing of Superior Reference Genes for Transcript Normalization in Arabidopsis. *Plant Physiol.* **2005**, *volume 139*, pp. 5–17, doi: 10.1104/pp.105.063743.

65 Carrasco-Loba, V.; Pollmann, S., Highly Sensitive Salicylic Acid Quantification in Milligram Amounts of Plant Tissue. *Plant Hormones: Methods and Protocols*, J. Kleine-Vehn and M. Sauer, Eds. Springer New York,USA. **2017**, *volume 1497*, pp. 221–229. doi: 10.1007/978-1-4939-6469-7_18.

66 Chen, Y.-A.; Wen, Y.-C.; Chang, W.-C., AtPAN: An Integrated System for Reconstructing Transcriptional Regulatory Networks in Arabidopsis Thaliana. *BMC Genomics* **2012**, *volume 13*, p. 85, doi: 10.1186/1471-2164-13-85.

67 Lescot, M.; Déhais, P.; Thijs, G.; Marchal, K.; Moreau, Y.; *et al.*, PlantCARE, a Database of Plant Cis-Acting Regulatory Elements and a Portal to Tools for in Silico Analysis of Promoter Sequences. *Nucleic Acids Res.* **2002**, *volume 30*, pp. 325–7, doi: 10.1093/nar/30.1.325.

68 Curtis, M. D.; Grossniklaus, U., A Gateway Cloning Vector Set for High-Throughput Functional Analysis of Genes in Planta. *Plant Physiol.* **2003**, *volume 133*, pp. 462–469, doi: 10.1104/pp.103.027979.

69 Ehlert, A.; Weltmeier, F.; Wang, X.; Mayer, C. S.; Smeekens, S.; *et al.*, Two-Hybrid Protein-Protein Interaction Analysis in Arabidopsis Protoplasts: Establishment of a Heterodimerization Map of Group C and Group S BZIP Transcription Factors. *Plant J.* **2006**, *volume 46*, pp. 890–900, doi: 10.1111/j.1365-313X.2006.02731.x.

70 Weltmeier, F. *et al.*, Combinatorial Control of Arabidopsis Proline Dehydrogenase Transcription by Specific Heterodimerisation of BZIP Transcription Factors. *EMBO J.* **2006**, *volume 25*, pp. 3133–3143, doi: 10.1038/sj.emboj.7601206.

71 Ma, L.; Lukasik, E.; Gawehns, F.; Takken, F. L. W., The Use of Agroinfiltration for Transient Expression of Plant Resistance and Fungal Effector Proteins in Nicotiana Benthamiana Leaves. *Plant Fungal Pathogens: Methods in Molecular Biology*, Bart P.H.J Thomma and Melvin D. Bolton, Eds. Humana Press, Springer, USA, **2012**, *volume 835*, pp. 61–74. doi: 10.1007/978-1-61779-501-5_4.

72 Jefferson, R. A.; Kavanagh, T. A.; Bevan, M. W., GUS Fusions: Beta-Glucuronidase as a Sensitive and Versatile Gene Fusion Marker in Higher Plants. *EMBO J.* **1987**, *volume 6*, pp. 3901–3907, doi: 10.1002/j.1460-2075.1987.tb02730.x.

73 Kirby, J.; Kavanagh, T. A., NAN Fusions: A Synthetic Sialidase Reporter Gene as a Sensitive and Versatile Partner for GUS. *Plant J.* **2002**, *volume 32*, pp. 391–400, doi: 10.1046/j.1365-313X.2002.01422.x.

74 Bradford, M. M., A Rapid and Sensitive Method for the Quantitation of Microgram Quantities of Protein Utilizing the Principle of Protein-Dye Binding. *Anal. Biochem.* **May 1976**, *volume 72*, pp. 248–254, doi: 10.1016/0003-2697(76)90527-3.

75 Sprenger-Haussels, M.; Weisshaar, B., Transactivation Properties of Parsely Proline-Rich BZIP Transcription Factors. *Plant J.* **2000**, *volume 22*, pp. 1–8.

76 Earley, K. W. *et al.*, Gateway-Compatible Vectors for Plant Functional Genomics and Proteomics. *Plant J.* **2006**, *volume 45*, pp. 616–629, doi: 10.1111/j.1365-313X.2005.02617.x.

77 Mathur, J.; Koncz, C., PEG-Mediated Protoplast Transformation with Naked DNA. *Methods Mol. Biol.* **1998**, *volume 82*, pp. 267–76, doi: 10.1385/0-89603-391-0:267.

78 Yoo, S.-D.; Cho, Y.-H.; Sheen, J., Arabidopsis Mesophyll Protoplasts: A Versatile Cell System for Transient Gene Expression Analysis. *Nat. Protoc.* **2007**, *volume 2*, pp. 1565–1572, doi: 10.1038/nprot.2007.199.

79 Alonso, R.; Oñate-Sánchez, L.; Weltmeier, F.; Ehlert, A.; Diaz, I.; *et al.*, A Pivotal Role of the Basic Leucine Zipper Transcription Factor BZIP53 in the Regulation of Arabidopsis Seed Maturation Gene Expression Based on Heterodimerization and Protein Complex Formation. *Plant Cell* **2009**, *volume 21*, pp. 1747–1761, doi: 10.1105/tpc.108.062968.

80 Gallagher, S. R., Quantitation of GUS Activity by Fluorometry. , *GUS Protocols. Using the GUS gene as a reporter of gene expression*, ACADEMIC PRESS, INC., USA, **1992**, pp. 47–59. doi: 10.1016/B978-0-12-274010-7.50009-4.

81 Cazaux, M. *et al.*, Application of Two-Spotted Spider Mite Tetranychus Urticae for Plant-Pest Interaction Studies. *J. Vis. Exp.* **2014**, p. e51738, doi: 10.3791/51738.